Fluctuations of light scattered by fractal clusters

Vadim A. Markel, Vladimir M. Shalaev, and Evgeni Y. Poliakov

Department of Physics, New Mexico State University, Las Cruces, New Mexico 88003

Thomas F. George

Office of the Chancellor/Departments of Chemistry, Physics, and Astronomy, University of Wisconsin–Stevens Point, Stevens Point, Wisconsin 54481-3897

Received April 18, 1996; revised manuscript received August 20, 1996; accepted August 28, 1996

Fluctuations in light scattering from a finite ensemble of fractal clusters are studied numerically and theoretically. It is shown that, for a wide range of wavelengths and angles, relative fluctuations in the scattered intensity are very close to 1 and do not depend on the number of monomers N in fractal clusters (whereas they are proportional to $1/\sqrt{N}$ for trivial clusters). The relations describing fluctuations in the light scattering are suggested; one can use them to extract important information about properties and parameters of fractal pollutants in the atmosphere. © 1997 Optical Society of America.

1. INTRODUCTION

Optical methods for remote detection and characterization of air pollution have attracted much attention.[1–3] Most of the optical methods are based on measuring the intensity of scattered light and its angular and spectral dependence[2,3] and depolarization.[4] Multiwavelength techniques[5,6] have been used for sensing of polydisperse aerosols. However, the data obtained as a result of such measurements do not provide complete information about the pollution. In this paper we suggest that measurements of fluctuations of the intensity of scattered light can provide additional equations that are necessary to extract the missing parameters.

During the past two decades it has become clear that in many cases the particles of sooty smoke, which is lofted into the atmosphere, possess geometrical properties of fractal clusters. They are built from many hundreds or even thousands of smaller particles (monomers), which aggregate and stick together to form submicron and micron fractal clusters.[2,3,7]

The average intensity of light scattered from fractal clusters has been investigated, for instance, in Refs. 8 and 9. It has been shown that the scattered light intensity, $I(q)$, bears information about the fractal dimension, D, of clusters,

$$I(q) \sim q^{-D},$$

where $\mathbf{q} = \mathbf{k} - \mathbf{k}'$ is the transmitted wave vector. One can also use the magnitude of the scattered intensity to find the average density of the scattering material. Though this result is useful, it does not allow one to extract some important parameters of fractal clusters, such as the number of monomers in clusters and the characteristic geometrical size of clusters.

Here we propose to use more subtle measurements, namely, the measurements of the fluctuations of the scattered light. Based on numerical and theoretical results, we show that these fluctuations are much different for scattering from fractal and nonfractal (trivial) clusters and can provide additional information about the nature and the geometry of scattering objects.

All results reported in this paper are based on the mean-field approximation (MFA) described, for example, in Ref. 8. This approximation is accurate for nonresonant light scattering, which is usually the case for scattering from carbon clusters in the optical region of the spectrum. (Resonant light scattering by fractals was considered in Ref. 10, and fluctuations of local fields in fractals under resonant excitation were studied in Ref. 11.)

This paper is organized as follows. In Section 2 we review the basic geometrical properties of fractal clusters and describe computer models that we have used for simulation of fractal and trivial clusters. In Section 3 we review the MFA. Our main results for fluctuations of light scattered by mono- and polydisperse ensembles of fractal clusters are presented in Sec. 4. In Section 5 we compare the results obtained for fractal and nonfractal clusters. Finally, in Section 6 we briefly discuss main results of the paper.

2. GEOMETRICAL PROPERTIES OF FRACTAL CLUSTERS

In this section we summarize general geometrical properties of fractal clusters and describe computer models that we use for simulation of real soot aggregates in the atmosphere.

A. General Properties

We consider an ensemble of clusters containing N pointlike particles (monomers). One can define a characteristic cluster size in different ways. The radius of gyration, R_g, for example, is defined as

$$R_g^2 = \langle (\mathbf{r} - \mathbf{R}_{cm})^2 \rangle, \quad (1)$$

0740-3232/97/010001-11$10.00

where $\mathbf{r}$ is the coordinate of a monomer in a cluster, $\mathbf{R}_{cm}$ is the coordinate of the center of mass of the cluster, and $\langle\ \rangle$ denotes averaging over an ensemble of clusters. Another possible choice for the characteristic size is the root-mean-square distance between monomers, R_{rms}, i.e., $\sqrt{2}$ times the radius of gyration.

The most simple definition of the fractal dimension D is through the relation between the radius of gyration and the number of particles in a cluster,

$$N = (R_g/R_0)^D, \tag{2}$$

where R_0 is a constant of length of the order of the minimum separation between particles. In practice, this relation is not very useful because, in order to calculate D, one needs to build a large number of clusters with different N. A more practical definition for the fractal dimension uses the pair correlation function, $p_2(r)$, which is an ensemble-average probability density of finding a pair of monomers (belonging to the same cluster) at the distance r from each other:

$$p_2(r) = ar^{D-1}/N \qquad \text{if } R_0 \ll r \ll R_c. \tag{3}$$

Hereafter, by R_c we imply any of the characteristic cluster sizes, R_g or R_{rms} (when it is needed, we specifically refer to R_g or R_c). The constant a appearing in Eq. (3) is N independent but can be different for different classes of fractals. It should be noted that there is no obvious way to relate the constants a and R_0, since the number of particles lying within the radius of gyration varies from cluster to cluster.

B. Numerical Simulations of Fractal Clusters

In our numerical simulations we used random ensembles of computer-generated fractal clusters. The computer model of cluster–cluster aggregation (CCA) (Ref. 13) well reproduces geometrical properties of real fractal clusters formed in the atmosphere, under the condition that there is no space-fixed center of aggregation and the concentration of the aggregating material is low. These conditions are usually well fulfilled. (For a detailed description of the CCA algorithm see, for example, Ref. 13.)

We used the CCA model to build two ensembles of random fractal clusters. The first ensemble was monodisperse and consisted of 40 clusters containing 10,000 monomers each. The clusters were built on a simple cubic lattice with dimension $300 \times 300 \times 300$ and periodic boundary conditions. In the numerical calculations we used the lattice unit as a unit of length, so that all physical quantities of dimensionality of length (such as a wavelength λ) are measured in lattice units.

The values of characteristic cluster sizes for the ensemble were $R_g = 70.3$ and $R_{rms} = 99.4$. The value of R_0 determined from Eq. (2) and the above value of R_g was 0.4.

The size of the lattice was chosen so that the average concentration of monomers is low enough ($\approx 4 \times 10^{-4}$ monomers per site) and the maximum size of clusters is smaller than the size of the lattice. This ensures that the clusters manifest well the fractal morphology, with the correct form of the function $p_2(r)$ (see Fig. 1). The values $D = 1.78$ and $a = 4.12$ for the asymptote (3) in Fig. 1 are found from the linear regression. Our result for D is in good agreement with the commonly accepted value of D for CCA clusters.

The second ensemble of clusters that we built was polydisperse and consisted of 100 clusters. The number of particles in clusters was distributed according to the Gaussian probability distribution with the average $\langle N\rangle = 5000$ and the dispersion $\sigma_N = \sqrt{\langle N^2\rangle - \langle N\rangle^2} = 2000$.[14] The dimension of the lattice, L, was adjusted for each cluster according to $L(N) = 300(N/10^4)^{1/D}$. This provided the same relation between R_c and L for all clusters (this relation was also valid for the monodisperse ensemble).

In order to compare results for fractal and nonfractal (trivial) clusters, we also generated an ensemble of random clusters with $D = 3$. We used the algorithm of randomly close-packed hard spheres (CPHS). In this algorithm one chooses first a volume to be occupied by a cluster. In our simulations it was a sphere, since we intended to build clusters that are spherically symmetric, on average. Then monomers are randomly placed inside the volume. At each step the intersection condition is checked: If the newly placed monomer approaches any of the previously placed monomers closer than the unit distance, this step is rejected and the next random position is tried. In this way each monomer can be thought of as a hard sphere of radius 1/2. The procedure stops when a large number of tries is consequently rejected. In our simulations this number was chosen to be 2×10^7.

This algorithm allows one to achieve a fairly dense package. As the volume to be occupied by a cluster, we chose a spherical volume with radius 14.2 and consequently packed in it 40 different clusters with an average of 9200 monomers per cluster. The volume fraction occupied by particles (of the volume $\pi/6$ each) was $\approx$0.40. (For comparison, it is $\approx$0.52 in the case of a simple cubic lattice and can be even lower for some other types of lattice.) In these clusters the minimum distance between

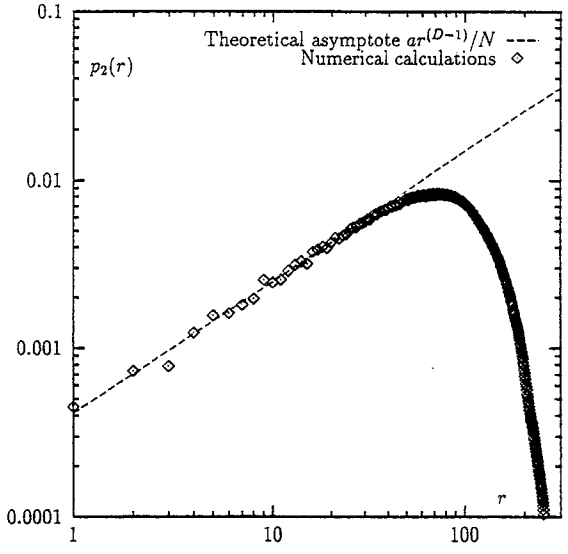

Fig. 1. Two-point correlation function, $p_2(r)$.

neighbor monomers was very close to 1; the maximum distance varied from 1.2 to 1.3.

Although the CPHS clusters were not completely monodisperse, the variation of N was very small: The ratio of the standard deviation of N to the mean was equal to 2.4×10^{-3}.

3. REVIEW OF THE MEAN-FIELD APPROXIMATION

The results presented below are based on the MFA applied first by Berry and Percival for the description of optical properties of fractals.[8] The main feature of the MFA to be used below is the assumption that the phases of dipole moments of all monomers coincide with the phases of the incident wave. In this section we briefly review the MFA and recapitulate the important relations that will be used in subsequent sections.

A. Formulation of the Mean-Field Approximation

Consider a cluster of N small polarizable spherules (monomers) located in space at points $\mathbf{r}_i$, $i = 1, \ldots, N$. For simplicity, we assume that all the particles are identical and possess a scalar dipole polarizability α. The cluster is irradiated by a plane monochromatic wave,

$$\mathbf{E}(\mathbf{r}, t) = \mathbf{E}_0 \exp(i\mathbf{k} \cdot \mathbf{r} - i\omega t), \tag{4}$$

which induces dipole momenta $\mathbf{d}_i$ in each particle.

A theoretical basis for building the MFA involves the equations that couple all the dipole moments in a cluster to the field of the incident wave (4) and to each other. These equations, known as the coupled-dipole equation, have the following form:

$$\mathbf{d}_i = \alpha\left[\mathbf{E}_0 \exp(i\mathbf{k} \cdot \mathbf{r}_i) + \sum_{\substack{j=1 \\ j\neq i}}^{N} \hat{W}(\mathbf{r}_i - \mathbf{r}_j) \circ \mathbf{d}_j\right]. \tag{5}$$

The second term on the right-hand side of Eq. (5) describes the interactions of dipoles with each other; $\hat{W}(\mathbf{r}_i - \mathbf{r}_j) \circ \mathbf{d}_j$ is simply the electric field produced by the jth dipole at the point where the ith dipole is located [the βth component of this field is $\Sigma_\gamma \hat{W}_{\beta\gamma}(\mathbf{r}_i - \mathbf{r}_j)d_{j,\gamma}$]. The exact form of the tensor $\hat{W}$ is defined by general formulas for the dipole radiation (see, for example, Ref. 15):

$$W_{\alpha\beta}(\mathbf{r}) = A(kr)\delta_{\alpha\beta} + B(kr)\frac{r_\alpha r_\beta}{r^2}, \tag{6}$$

$$A(x) = (x^{-1} + ix^{-2} - x^{-3})\exp(ix), \tag{7}$$

$$B(x) = (-x^{-1} - 3ix^{-2} + 3x^{-3})\exp(ix). \tag{8}$$

Here the Greek indices stand for the Cartesian components of vectors, and $A(x)$ and $B(x)$ are complex functions of a real scalar argument.

In the MFA the dipole moments are given by[8]

$$\mathbf{d}_i = \frac{\mathbf{E}_0 \exp(i\mathbf{k} \cdot \mathbf{r}_i)}{1/\alpha - (N-1)Q}, \tag{9}$$

where the factor Q is defined as

$$Q = \frac{\langle[\mathbf{E}_0 \cdot \hat{W}(\mathbf{r}_i) - \mathbf{r}_j) \circ \mathbf{E}_0]\exp[i\mathbf{k} \cdot (\mathbf{r}_j - \mathbf{r}_i)]\rangle}{|\mathbf{E}_0|^2}, \tag{10}$$

and $\langle\ \rangle$ denotes ensemble averaging over all possible distances $\mathbf{r}_i - \mathbf{r}_j$ between distinct monomers ($i \neq j$) in a cluster. Note that, for an ensemble of spherically symmetrical (on average) clusters, the dependence of Q on $\mathbf{E}_0$ vanishes, since the off-diagonal elements of $\hat{W}$ turn out to be zeros after the averaging.

It should be noted that the MFA is always correct in the case of a homogeneous (on average) continuous medium, since in this case Eq. (9) is the eigenvector of the operator of translation. Clusters, however, do not possess translational symmetry. So we can say that the MFA neglects the geometrical structure of clusters for the purpose of the calculation of phases of dipole moments, effectively replacing a cluster by a continuous medium, but it does consider the geometry for calculating amplitudes of dipole moments.

In principle, the MFA allows one to take into account all the orders of the multiple scattering. If the multiple scattering is not essential, as in the limit $|\alpha w_n| \ll 1$ (off-resonance excitation), the MFA coincides with the first Born approximation.

B. Multiple Scattering

Below we consider two different ensembles of clusters, monodisperse and polydisperse. In monodisperse systems the number of particles is the same for all clusters, whereas it is different for polydisperse systems.

For fluctuations in light scattering from a monodisperse ensemble of clusters the value of the parameter $(N-1)Q \approx NQ$ appearing in Eq. (9) is not important because it is the same for all clusters. Since Q is defined as an ensemble average, we could generalize its definition to the case of a polydisperse ensemble. We can think of a polydisperse ensemble as a set of monodisperse subensembles with different N. Each of these subensembles would be characterized by its own value of NQ, and, if NQ depends on N, it would clearly contribute to the fluctuations. This fact would complicate consideration of fluctuations of scattered light in a polydisperse ensemble of clusters.

There are two important cases in which we can neglect this effect and consider NQ as independent of N and the same for all clusters. The first trivial case corresponds to the limit of small $N\alpha Q$, where we can use the first Born approximation (simply by setting $Q = 0$). Since Q depends on N, the above condition is actually N dependent and can be, in principle, violated for very large N, even if α is very small. Thus a very thick layer of a fairly transparent material may become eventually optically dense. But in many cases this condition can be well fulfilled for nonresonant excitation of submicron clusters.

The second condition is not as trivial. As was pointed out by Berry and Percival,[8] NQ does not depend on N for $D < 2$. A physical interpretation of this effect is that a cluster with $D < 2$ stays geometrically transparent when N increases toward infinity. This fact can also be understood from a mathematical point of view.[8]

We first rewrite the definition (10) of Q in terms of the pair correlation function, $p_2(r)$, by using the expression (6) for $\hat{W}$:

$$Q = \int_0^\infty p_2(r)\mathrm{d}r \int_0^\pi \int_0^{2\pi} [A(kr) + B(kr)\sin^2\theta\cos^2\phi]\exp(ikr\cos\theta)\frac{\sin\theta\,\mathrm{d}\theta\mathrm{d}\phi}{4\pi}, \tag{11}$$

where A and B are defined by Eqs. (7) and (8). After integrating over θ and ϕ, we have

$$Q = \int_0^\infty \frac{p_2(r)}{kr}\left\{A(kr)\sin(kr) - \frac{1}{kr}\left[\cos(kr) - \frac{\sin(kr)}{kr}\right]B(kr)\right\}\mathrm{d}r. \tag{12}$$

Since $p_2(r) \propto 1/N$ for small r, we can state that NQ does not depend on N if the integral in Eq. (12) converges at distances smaller than the size of a cluster, i.e., $r < R_c$ [when the asymptote (3) is still valid]. In order to check the convergence, we consider the term that decays most slowly in the integrand of Eq. (12). This term comes from the first term in $A(kr)$ [Eq. (7)] and is proportional to $r^{-2}\sin(kr)\exp(ikr)$. For $r \ll R_c$ we can replace $p_2(r)$ by its asymptotic form (3), and the corresponding integral acquires the form

$$\frac{1}{N}\int r^{D-3}\sin(kr)\exp(ikr)\mathrm{d}r = \frac{1}{N}\int r^{D-3}\frac{\exp(2ikr) - 1}{2i}\mathrm{d}r, \tag{13}$$

which clearly converges for $D < 2$ (and diverges if $D > 2$). This means that the value of NQ is defined only by the form of the asymptote (3), which is universal and does not depend on R_c and, consequently, on N.

We can say that the role of multiple scattering does not increase with N for $D < 2$. Thus, if the multiple scattering were negligible for small clusters (as it is in the case of off-resonance excitation), it would stay negligible for large clusters, no matter how many particles they contain. For the resonant excitation, multiple scattering can be significant for small clusters, even if there are only two monomers. But as N grows, the impact of multiple scattering remains the same for $D < 2$.

Since the cluster–cluster aggregates and, in particular, the smoke clusters have $D = 1.78 < 2$, the quantity NQ does not depend on N. But this is not the case for trivial (nonfractal) clusters with $D = 3$.

C. Scattering Cross Section

We can use the solutions to the coupled dipole equation (5) to write general expressions for the scattering amplitude and the optical cross sections in terms of dipole moments $\mathbf{d}_i$ (see, for example, Refs. 10 and 12). For a single cluster built of N particles the expression for the scattering amplitude $\mathbf{f}(\mathbf{s})$ is

$$\mathbf{f}(\mathbf{s}) = k^2\sum_{i=1}^{N}[\mathbf{d}_i - (\mathbf{d}_i\cdot\mathbf{s})\mathbf{s}]\exp(-ik\mathbf{s}\cdot\mathbf{r}_i), \tag{14}$$

where $\mathbf{s}$ is a unit vector in the direction of scattering and the wave vector of the scattered wave is $\mathbf{k}' = k\mathbf{s}$.

In the MFA this expression is simplified with the use of Eq. (9) to the form

$$\mathbf{f}(\mathbf{s}) = k^2\frac{\mathbf{E}_0 - (\mathbf{E}_0\cdot\mathbf{s})\mathbf{s}}{1/\alpha - (N-1)Q}\sum_{i=1}^{N}\exp(i\mathbf{q}\cdot\mathbf{r}_i), \tag{15}$$

where $\mathbf{q} = \mathbf{k} - \mathbf{k}'$. The differential scattering cross section is defined by

$$\frac{\mathrm{d}\sigma_s}{\mathrm{d}\Omega} = |\mathbf{f}(\mathbf{s})|^2 = \frac{k^4|\mathbf{E}_0|^2\sin^2[\psi(\mathbf{E}_0,\mathbf{s})]}{|1/\alpha - (N-1)Q|^2}\left|\times\sum_{i=1}^{N}\exp(i\mathbf{q}\cdot\mathbf{r}_i)\right|^2, \tag{16}$$

where $\psi(\mathbf{E}_0,\mathbf{s})$ denotes the angle between $\mathbf{E}_0$ and $\mathbf{s}$.

As mentioned in Subsection 3.B, the value of $(N-1)Q \approx NQ$ is the same for all clusters and does not depend on N for $D < 2$. Therefore the whole factor $k^4|\mathbf{E}_0|^2\sin^2[\psi(\mathbf{E}_0,\mathbf{s})]/|1/\alpha - (N-1)Q|^2$ is the same for all clusters. In contrast, the factor $|\Sigma_{i=1}^{N}\exp(i\mathbf{q}\cdot\mathbf{r}_i)|^2$ in Eq. (16) is random and can vary from cluster to cluster.

When considering fluctuations of scattered light by different random clusters, we do not need to keep a factor that is common to all of them. Therefore it is convenient to define the intensity of the light scattered by some individual cluster as

$$I(\theta,\phi) = I(\mathbf{q}) = \left|\sum_{i=1}^{N}\exp(i\mathbf{q}\cdot\mathbf{r}_i)\right|^2, \tag{17}$$

where ϕ is the azimuthal angle and the absolute value of $\mathbf{q}$ depends on the scattering angle θ as

$$q = k\sqrt{2(1-\cos\theta)}. \tag{18}$$

In the case of scattering of a depolarized wave we must replace $\sin^2[\psi(\mathbf{E}_0,\mathbf{s})]$ by $\langle\sin^2\psi\rangle = 1 - (1/2)\cos^2\theta$. Though there still is a dependence on the scattering angle in the prefactor of Eq. (16), the dependence on the azimuthal angle ϕ is eliminated after such averaging.

The intensity (17) coincides with the real intensity of the scattered light up to some function of θ in the case of a depolarized incident wave and up to some function of θ and ϕ for a polarized wave. Note that the definition of the intensity in Eq. (17) is suitable only for the calculation of *relative* fluctuations, i.e., for the dispersion of scattered intensity divided by the average scattered intensity. If we want to calculate *absolute* fluctuations, we need, of course, to keep all the prefactors.

In this paper we focus on relative fluctuations. The absolute value of fluctuations can always be reconstructed, provided that the average scattered intensity is known.

4. FLUCTUATIONS OF LIGHT SCATTERED BY FRACTAL CLUSTERS

A. General Relations

Below we consider the intensity of light scattered by some number of fractal clusters randomly distributed in some volume. The distance between clusters is supposed to be large compared with the wavelength of the incident radiation, λ, and the distribution of clusters in space is supposed to be random and uncorrelated. Then we can add the intensities of light scattered by each cluster, rather than the amplitudes.

The average scattered intensity $\langle I \rangle$ is defined as

$$\langle I \rangle = \langle I(\theta, \phi) \rangle = \lim_{M \to \infty} \frac{1}{M} \sum_{k=1}^{M} I_k(\theta, \phi), \tag{19}$$

where $I_k(\theta, \phi)$ is the intensity scattered by the kth cluster; M is the total number of clusters that scatter the light; θ, as above, is the angle between the direction of the incident wave vector $\mathbf{k}$ and the direction of scattering; and ϕ is the azimuthal angle. With the use of Eq. (17) we can rewrite Eq. (19) as

$$\langle I \rangle = \lim_{M \to \infty} \frac{1}{M} \sum_{k=1}^{M} \sum_{i,j=1}^{N_k} \exp\{i\mathbf{q} \cdot [\mathbf{r}_i^{(k)} - \mathbf{r}_j^{(k)}]\}, \tag{20}$$

where N_k is the number of monomers in the kth cluster and $\mathbf{r}_i^{(k)}$ is the coordinate of the ith monomer in the kth cluster.

For an ensemble of spherically symmetrical (on average) clusters the dependence of $\langle I \rangle$ on ϕ is weak (it vanishes for an infinite ensemble); therefore we will use the notation $\langle I \rangle = \langle I(\theta) \rangle = \langle I(q) \rangle$, where q is defined by Eq. (18).

If we detect the scattered light from just one cluster, it can be much different from $\langle I \rangle$. A convenient measure of these variations is the standard deviation (dispersion), σ_I:

$$\sigma_I^2 = \langle I^2 \rangle - \langle I \rangle^2. \tag{21}$$

The value of σ_I characterizes possible deviations of I_k from $\langle I \rangle$ calculated for an infinite ensemble of clusters and has a simple mathematical meaning: The probability that an individual I_k lies within the interval $\langle I \rangle \pm \sigma_I$ is approximately 2/3.

In the case of a finite M one can be interested in a measure of fluctuations of the average value (19) itself [the lim sign in this case should, of course, be omitted in Eqs. (21) and (22)]. If we register the scattered light from different ensembles of clusters consisting of some finite number of clusters M, we will come up with different results. We can define the standard deviation $\sigma_I^{(M)}$ of these random values in the usual way. The relation between $\sigma_I^{(M)}$ and $\sigma_I \equiv \sigma_I^{(1)}$ is well known from mathematical statistics:

$$\sigma_I^{(M)} = \frac{\sigma_I}{\sqrt{M}}. \tag{22}$$

The actual value of M depends on the scheme of the experiment. In one possible setting the scattering volume is small enough (e.g., as a result of focusing a laser beam) and contains only one cluster at a time. Because of the random motion of clusters, the volume contains different clusters in different moments of time. In this case one can register scattered radiation for some large period of time (excluding the periods when the volume contains no clusters at all and the signal is zero) and calculate the time-averaged intensity and its standard deviation, which coincides with σ_I. If the volume contains, on average, M clusters at a given time, the measured standard deviation would be $\sigma_I^{(M)}$.

Here we focus on the calculation of the relative dispersion $\sigma_I/\langle I \rangle$. As will be shown numerically in Subsection 4.B, this value is universal for CCA clusters in a wide range of scattering angles. We can use relation (22) to find the average number of clusters in the scattering volume (and, hence, the number density of clusters).

B. Monodisperse Clusters

First, we consider monodisperse ensembles of clusters consisting of N monomers each. The task of calculating σ_I includes finding two average values: $\langle I \rangle$ and $\langle I^2 \rangle$. The first of them has an independent virtue and is experimentally measurable.

Berry and Percival[8] showed that one can use the asymptotic form (3) for the pair correlation function $p_2(r)$ to calculate $\langle I \rangle$. Indeed, for a monodisperse ensemble, Eq. (20) can be simplified to

$$\langle I \rangle = N + N(N-1)\langle \exp(i\mathbf{q} \cdot \mathbf{r}_{ij}) \rangle, \tag{23}$$

where $\mathbf{r}_{ij} = \mathbf{r}_i - \mathbf{r}_j$, and only distinct monomers belonging to the same cluster are considered, i.e., $i \neq j$ (the superscripts in $\mathbf{r}_i$ and $\mathbf{r}_j$ are omitted). Now we can use the function $p_2(r)$ to calculate $\langle \exp(i\mathbf{q} \cdot \mathbf{r}_{ij}) \rangle$:

$$\langle \exp(i\mathbf{q} \cdot \mathbf{r}_{ij}) \rangle = \int_0^\infty p_2(r) \exp(i\mathbf{q} \cdot \mathbf{r}_{ij}) \frac{\mathrm{d}r \sin\theta \, \mathrm{d}\theta \mathrm{d}\phi}{4\pi}. \tag{24}$$

After the angular integration is performed, Eq. (24) simplifies to

$$\langle \exp(i\mathbf{q} \cdot \mathbf{r}_{ij}) \rangle = \int_0^\infty p_2(r) \frac{\sin(qr)}{qr} \mathrm{d}r. \tag{25}$$

In the case $D < 2$ and $q \gg R_c^{-1}$ the integral (25) converges at the distances for which the asymptote (3) is still valid. The final result of the integration is

$$\langle \exp(i\mathbf{q} \cdot \mathbf{r}_{ij}) \rangle = \frac{a\Gamma(D-1)\sin[\pi(D-1)/2]}{Nq^D}. \tag{26}$$

If $q \ll R_c^{-1}$, $\sin(qr)$ can be expanded in a power series in Eq. (25), and the result of the integration up to the lowest nonzero power of q is

$$\langle \exp(i\mathbf{q} \cdot \mathbf{r}_{ij}) \rangle = 1 - (qR_{\mathrm{rms}})^2/6. \tag{27}$$

As follows from Eqs. (23) and (27), $\langle I(\theta = 0) \rangle = N^2$, which means that the forward scattering is always coherent in the frame of the MFA. From Eqs. (23) and (26) it can be concluded that the minimum possible value of $\langle I \rangle$ is N, which can be reached for large values of q. For the backscattering, when the value of q is maximum, the expression for $\langle I \rangle$ becomes $\langle I \rangle = N(1 + 5 \times 10^{-2}\lambda^D)$, where we used the numerical values for all the coeffi-

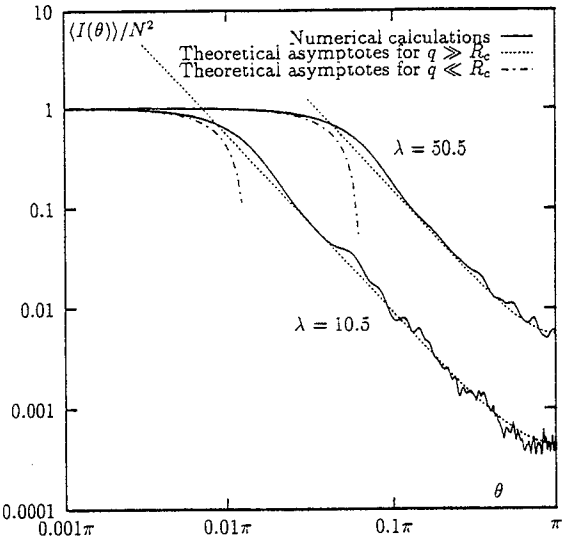

Fig. 2. Average intensity of the scattered light for $\lambda = 10.5$ and $\lambda = 50.5$ (lattice units).

cients. The characteristic value of λ is 5.4 lattice units, so that, for smaller λ, $\langle I\rangle$ can approach its lower bound. (But one should keep in mind that, for λ comparable with the lattice unit, clusters become essentially discrete systems, and the description based on a smooth function p_2 is no longer valid.)

The theoretical asymptotes (26) and (27), along with the results of numerical calculations for $\langle I\rangle$ for different values of λ, are illustrated in Fig. 2. (Note that we chose noninteger values of λ in order to avoid lattice effects.) In fact, the domains where these two asymptotes are valid come fairly close to each other. The threshold angles θ_c defined from the condition $q(\theta_c) = R_{\rm rms}^{-1}$ are $5.4 \times 10^{-3}\pi$ for $\lambda = 10.5$ and $2.6 \times 10^{-2}\pi$ for $\lambda = 50.5$.

Whereas $\langle I\rangle$ is well defined by $p_2(r)$, one needs a higher-order correlation function for the calculation of $\langle I^2\rangle$. Indeed, the definition of $\langle I^2\rangle$ analogous to Eq. (20) would contain a fourfold summation, which, after we group together the terms with different indices matching each other, turns into

$$\langle I^2\rangle = N(2N-1) + 4N(N-1)^2\langle\exp(i\mathbf{q}\cdot\mathbf{r}_{ij})\rangle + N(N-1)(N^2-3N+3)\langle\exp(i\mathbf{q}\cdot\mathbf{r}_{ijkl})\rangle, \tag{28}$$

where $\mathbf{r}_{ijkl} = \mathbf{r}_{ij} - \mathbf{r}_{kl}$, $i \neq j$, $k \neq l$, and any of the pair of indices (i, j) can coincide with any of the pair (k, l). It is easy to show that $\langle\exp(i\mathbf{q}\cdot\mathbf{r}_{ijkl})\rangle$ is expressed through the four-point correlation function, $p_4(r)$, which is defined as the probability density of finding the value of $\mathbf{r}_{ijkl}$ to be equal to r, exactly in the same form as that in Eq. (25), with $\mathbf{r}_{ij}$ replaced by $\mathbf{r}_{ijkl}$ and p_2 replaced by p_4.

Whereas the pair correlation function p_2 is well investigated, there is little information on the four-point correlation function p_4. We found numerically that, for small r, $p_4(r)$ scales like r^β, where β is very close to D. Consequently, the integral of the type of Eq. (25) would diverge if we replace the actual $p_4(r)$ by its small-r asymptote. This means that we require the exact form of $p_4(r)$ to calculate $\langle I^2\rangle$. We will report more detailed results on $p_4(r)$ elsewhere.

We now turn to numerical results for fluctuations. We calculated the value of $\sigma_I/\langle I\rangle$ as a function of scattering angle θ for the ensemble of 40 CCA clusters, with $N = 10{,}000$ monomers in each cluster. In this calculation we allowed θ to change from 0 to 2π, so that the observer makes a whole revolution from the forward direction of scattering to the backward direction and back to forward. In the usual spherical system of coordinates this corresponds to varying θ from 0 to π, then changing ϕ to $-\phi$ and varying it from π back to 0. Note that for a finite ensemble of random clusters the result is not necessarily symmetrical with respect to the point $\theta = \pi$. However, it must be symmetrical for an infinite ensemble of spherically symmetrical (on average) clusters; this follows from the fact that neither σ_I nor $\langle I\rangle$ can depend on ϕ in this case.

The results of the calculations are presented in Fig. 3. We first consider the domains of θ where the asymptote (26) is valid. The characteristic values of θ_c [defined from the condition $g(\theta_c) = R_{\rm rms}^{-1}$] are $5.4 \times 10^{-3}\pi$ for $\lambda = 10.5$, $1.0 \times 10^{-2}\pi$ for $\lambda = 20.5$, $2.6 \times 10^{-2}\pi$ for $\lambda = 50.5$, and 0.16π for $\lambda = 100.5$. One can easily see that the value of $\sigma_I/\langle I\rangle$ fluctuates near unity if $\theta_c \ll \theta \ll 2\pi - \theta_c$.[17] It should be noted that for a finite ensemble $\sigma_I/\langle I\rangle$ is a random quantity itself. Since there is no noticeable systematic dependence on θ in the domain defined above, we can perform additional averaging of $\sigma_I/\langle I\rangle$ over θ. The results for this averaging are (up to the third significant figure) 0.98 for $\lambda = 10.5$, 1.00 for $\lambda = 20.5$, 0.96 for $\lambda = 50.5$, and 1.01 for $\lambda = 100.5$.

The numerical data suggest that the value of relative fluctuations of the intensity of light scattered by CCA

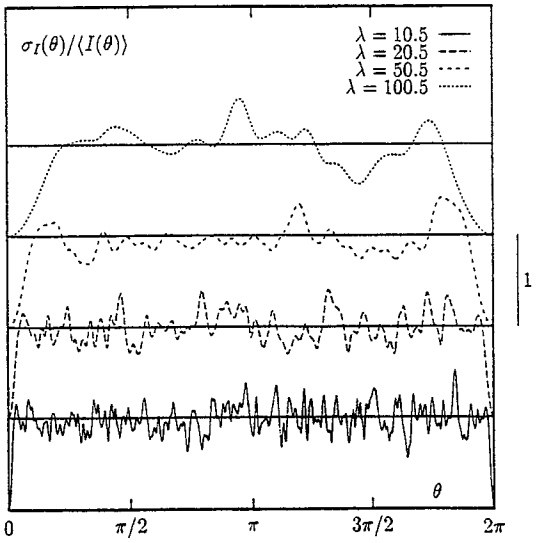

Fig. 3. Relative fluctuations $\sigma_I(\theta)/\langle I(\theta)\rangle$ for different wavelengths (CCA clusters; $D = 1.78$). For each curve the horizontal line corresponds to the level $\sigma_I/\langle I\rangle = 1$; the distance between the nearest horizontal lines is 1; $\sigma_I(0)/\langle I(0)\rangle = \sigma_I(2\pi)/\langle I(2\pi)\rangle = 0$.

clusters is very close to unity and statistically independent of the scattering angle θ as long as θ lies in the domain defined above. This is true for a wide range of wavelengths λ. However, for very large λ, the domain of θ shrinks and becomes essentially empty when $\lambda = 2\sqrt{2}\pi R_{\mathrm{rms}} \approx 9R_{\mathrm{rms}}$. For very small λ the lattice structure (or some characteristic interparticle distance in off-lattice clusters) would become of importance, leading to the appearance of sharp interference maxima and minima in the angular distribution of the intensity of scattered light.

Now we turn to the domain of small q (or, equivalently, small scattering angles). If q is much smaller than R_c^{-1}, we can expand the exponent in Eq. (17) so that the expression for the intensity scattered by the kth cluster up to the first nonvanishing power of q takes the form

$$I_k = N^2\left[1 - \frac{q^2}{2}\rho_k^2(\hat{\mathbf{q}})\right], \tag{29}$$

where

$$\rho_k^2(\hat{\mathbf{q}}) = \frac{1}{N^2}\sum_{i,j=1}^{N}[r_{ij}^{(k)}]^2\cos^2\{\psi[\mathbf{q}, \mathbf{r}_{ij}^{(k)}]\} \tag{30}$$

and $\hat{\mathbf{q}}$ is a unit vector in the direction of $\mathbf{q}$. We also used the limit of large N, namely, we put $N(N-1) = N^2$. Note that $\langle\rho_k^2(\hat{\mathbf{q}})\rangle = R_{\mathrm{rms}}^2/3$, so that Eq. (30) coincides with Eq. (27) after the averaging. However, an individual cluster can be not spherically symmetrical, which means that $p_k^2(\hat{\mathbf{q}})$ can depend on the direction of $\mathbf{q}$.

One can also use expression (30) to find $\langle I^2\rangle$ and, eventually, σ_I. The final result is

$$\frac{\sigma_I}{\langle I\rangle} = \frac{q^2}{2}\sqrt{\langle\rho^4\rangle - \langle\rho^2\rangle^2}. \tag{31}$$

Because of spherical symmetry, the dependence on the direction of $\mathbf{q}$ vanishes in the average quantities $\langle\rho^4\rangle$ and $\langle\rho^2\rangle$. Note that the above average values depend on N. As was mentioned above, $\langle\rho^2\rangle = R_{\mathrm{rms}}^2/3 \propto N^{2/D}$. Analogously, $\langle\rho^4\rangle \propto N^{4/D}$ and $\sigma_I/\langle I\rangle \propto N^{2/D}$ for a fixed value of $q \ll R_c^{-1}$. This is in agreement with the fact that the domain of q where $q \ll R_c^{-1}$ shrinks as N increases, but the value of $\sigma_I/\langle I\rangle$ becomes approximately equal to unity when $q > R_c^{-1}$. This means that the coefficient in front of q^2 in Eq. (31) should increase with increasing N.

C. Polydisperse Clusters

We now consider a polydisperse ensemble of clusters, i.e., an ensemble containing clusters with different N. We first look at the case of large q, when the condition $q \gg R_c^{-1}$ is fulfilled for almost every cluster in the ensemble.

We can calculate $\langle I\rangle$ by performing an additional averaging over N in Eq. (23). In the case of large q this averaging leads to

$$\langle I\rangle = \langle N\rangle\{1 + a\Gamma(D-1)\sin[\pi(D-1)/2]/q^D\}. \tag{32}$$

It is natural to assume that the intensity scattered by some individual cluster I_k can be represented as

$$I_k = N_k J_k, \tag{33}$$

where N_k and J_k are statistically independent random variables and

$$\langle J\rangle = 1 + a\Gamma(D-1)\sin[\pi(D-1)/2]/q^D. \tag{34}$$

Then an ensemble averaging in Eq. (33) results in Eq. (32).

For a monodisperse ensemble the J_k coincide with the I_k up to some constant, common for each cluster. Therefore the relative dispersion, $\sigma_J/\langle J\rangle$, coincides with the relative dispersion of I in a monodisperse ensemble.

Further, we can use Eq. (33) to calculate the relative dispersion of scattered intensity in a polydisperse ensemble in terms of that in a monodisperse ensemble and the dispersion of the random variable N. Straightforward algebra yields

$$\frac{\sigma_I}{\langle I\rangle} = \frac{\sigma_J}{\langle J\rangle}\sqrt{\frac{\sigma_N^2}{\langle N\rangle^2}\left(1 + \frac{\langle J\rangle^2}{\sigma_J^2}\right) + 1}. \tag{35}$$

From the numerical results of Subsection 4.B we know that $\sigma_J/\langle J\rangle$ is very close to unity. Substituting this value into Eq. (35), we obtain

$$\frac{\sigma_I}{\langle I\rangle} = \sqrt{2\frac{\sigma_N^2}{\langle N\rangle^2} + 1}. \tag{36}$$

It follows from formula (36) that $\sigma_I/\langle I\rangle$ is always close to unity, even for very polydisperse ensembles. The value of $\sigma_N/\langle N\rangle$ cannot be much larger than 1 for any physically reasonable distribution of N. For example, if N is uniformly distributed from 0 to N_{max}, this value is equal to $1/\sqrt{3}$. If the distribution has two sharp peaks of equal height near N_1 and N_2, it is equal to $|N_1 - N_2|/(N_1 + N_2)$. (The value of $\sigma_N/\langle N\rangle$ can be very large in a situation in which the distribution of N has a maximum near $N = 0$ and decays faster than exponentially with N.)

In order to verify Eq. (35), we calculated $\sigma_I/\langle I\rangle$ for a polydisperse ensemble of CCA clusters with $\sigma_N/\langle N\rangle = 0.37$ described in Section 2 for two different values of λ. After additional averaging over angles (as described in Subsection 4.B) the results obtained are as follows: $\sigma_I/\langle I\rangle = 1.109$ for $\lambda = 10.5$ and $\sigma_I/\langle I\rangle = 1.087$ for $\lambda = 20.5$. The results following from the theoretical formula (35) and the corresponding results for a monodisperse ensemble ($\sigma_J/\langle J\rangle$) are 1.109 and 1.120, respectively. As we can see, the results match closely. For the case of $\lambda = 10.5$ the difference is only in the fifth figure.

The results for the polydisperse ensemble also confirm indirectly the idea that $\sigma_I/\langle I\rangle$ is close to unity for any monodisperse ensemble, independent of N (provided that the condition for q is fulfilled). We could think that the result obtained numerically in Subsection 4.B concerns only clusters with $N = 10{,}000$ and that it is close to unity by chance. But in this subsection we confirmed this result for an ensemble with $\langle N\rangle = 5000$.

Now we turn to the domain of small q, where the above consideration is not valid. Experimentally, this domain of q can always be realized by a look at the forward scattering. We can use Eq. (29), with N replaced by N_k for the intensity scattered by the kth cluster. Further, since

all N_k are different, we do not need to consider the term proportional to q^2 in order to obtain the main contribution to $\sigma_I/\langle I\rangle$, that is,

$$\frac{\sigma_I}{\langle I\rangle} = \sqrt{\frac{\langle N^4\rangle - \langle N^2\rangle^2}{\langle N^2\rangle^2}}. \tag{37}$$

It is easy to verify that the first correction to this formula is also proportional to q^2.

Thus we see that, for the forward scattering, fluctuations of the number of monomers in clusters define fluctuations of the scattered light, whereas, for large q, the differences in the geometrical structures of clusters play a decisive role. This is natural, since in the MFA the forward scattering is always coherent.

5. FLUCTUATIONS OF LIGHT SCATTERED BY TRIVIAL CLUSTERS

It is interesting to compare the fluctuations of light scattered by fractal and by trivial ($D = 3$) clusters. For this purpose we generated on a computer the ensemble of CPHS clusters described in Subsection 2.B. In this section we limit ourselves to consideration of only monodisperse ensembles of clusters.

A. Numerical Results

The results of numerical simulations of $\sigma_I/\langle I\rangle$ for the ensemble of 40 CPHS clusters are shown in Fig. 4(a). As in Section 4, the scattering angle θ varies from 0 to 2π. First, we notice the strong and systematic dependence of $\sigma_I/\langle I\rangle$ on θ. For fractal clusters this dependence looks much like a statistical noise (cf. Fig. 3). Second, for most angles the value of $\sigma_I/\langle I\rangle$ is significantly less than 1 and decreases when λ grows. This dependence on λ is anticipated, because, for many monomers in the volume λ^3, a cluster becomes optically similar to a dielectric sphere, and its random structure is of no importance. But this is not the case for fractal clusters; they are geometrically different and random in all scales up to the maximum scale R_c. As seen from Fig. 3, $\sigma_I/\langle I\rangle$ for fractal clusters is of the order of 1, even for $\lambda = 100.5$. But for CPHS clusters $\sigma_I/\langle I\rangle$ is much less, of the order of 10^{-2} for $\lambda = 50.5$.

The second feature is the presence of sharp maxima in $\sigma_I/\langle I\rangle$ when it becomes of the order of 1. These maxima occur for the angles θ at which $\langle I(\theta)\rangle$ has minima [see Fig. 4(b)]. We explain this in more detail in Subsection 5.B.

Note also that $\sigma_I/\langle I\rangle$ does not turn exactly to zero when $\theta = 0$ and 2π. This is because the ensemble of the CPHS clusters is not exactly monodisperse (see Subsection 2.B).

B. Theoretical Results

The problem of fluctuations can be solved exactly for spherically symmetrical random clusters, provided that the positions of monomers in clusters are absolutely uncorrelated. This is not the case for the CPHS clusters, because in the CPHS model monomers cannot approach each other closer than the unit distance, which brings about short-range correlations. It is clear that the model of totally uncorrelated clusters (random gas) is not exact, since monomers act like hard spheres during aggregation. However, theoretical results for uncorrelated clusters help to explain the main features shown in Fig. 3.

We consider a random gas of uncorrelated particles inside a spherical volume of radius b. The ensemble-average quantities $\langle\exp(i\mathbf{q}\cdot\mathbf{r}_i)\rangle$, $\langle\exp(i\mathbf{q}\cdot\mathbf{r}_{ij})\rangle$, and $\langle\exp(i\mathbf{q}\cdot\mathbf{r}_{ijkl})\rangle$ can be obtained from straightforward integration and are as follows:

$$\langle\exp(i\mathbf{q}\cdot\mathbf{r}_i)\rangle = \varphi(qb) \equiv \frac{3}{(qb)^3}[\sin(qb) - qb\,\sin(qb)], \tag{38}$$

$$\langle\exp(i\mathbf{q}\cdot\mathbf{r}_{ij})\rangle = \varphi^2(qb), \tag{39}$$

$$\langle\exp(i\mathbf{q}\cdot\mathbf{r}_{ijkl})\rangle = \varphi^4(qb). \tag{40}$$

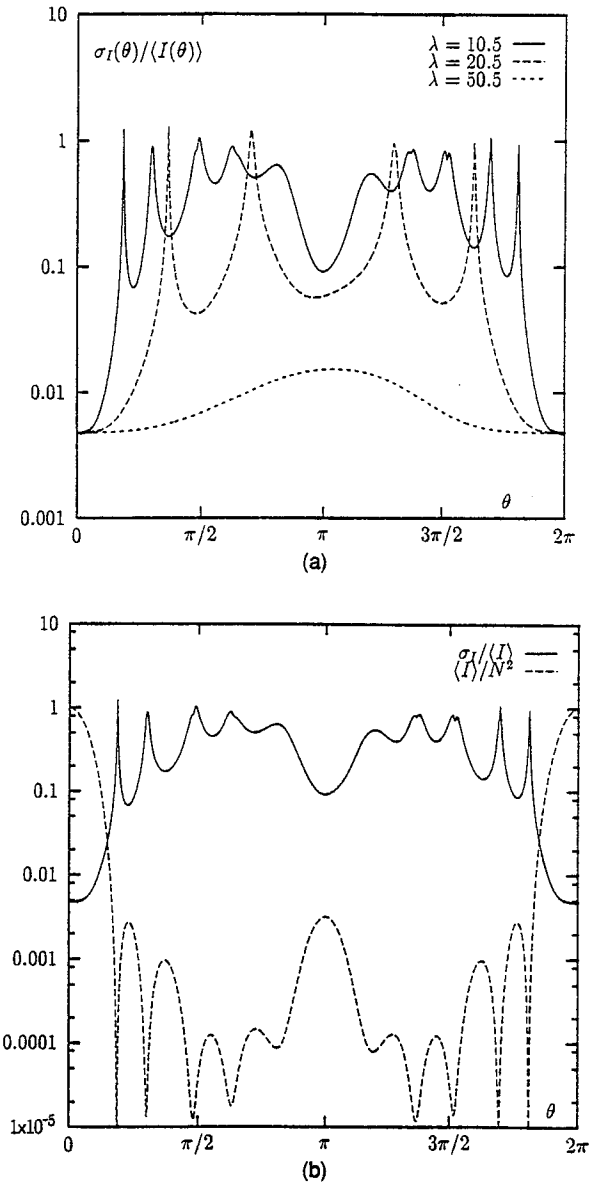

Fig. 4. (a) Relative fluctuations $\sigma_I(\theta)/\langle I(\theta)\rangle$ for different wavelengths (CPHS clusters; $D = 3$), (b) relative fluctuations, $\sigma_I(\theta)/\langle I(\theta)\rangle$, compared with the average scattered intensity $\langle I\rangle$ for $\lambda = 10.5$ (CPHS clusters).

The values of $\langle I\rangle$ and $\langle I^2\rangle$ can be found according to Eqs. (23) and (28) with the use of Eqs. (38)–(40). The expression for $\langle I\rangle$ is

$$\langle I\rangle = N + N(N-1)\varphi^2(qb), \tag{41}$$

and the expression for $\sigma I/\langle I\rangle$ is (in the limit of large N)

$$\frac{\sigma_I}{\langle I\rangle} = \frac{\sqrt{1 - 4\varphi^2 + 3\varphi^4 + 2\varphi^2(1-\varphi^2)N}}{1 + \varphi^2 N}. \tag{42}$$

If $\varphi(qb)$ turns to zero for some value of q, this means that $\sigma_I/\langle I\rangle$ has a maximum and is of the order of 1 for this q. At the same time the average scattered intensity (41) has a minimum.

The function $\varphi(x)$ turns exactly to zero at $\tan x = x$. The first root of this equation is $x \approx 1.43\pi$. The corresponding scattering angle is defined by $\cos\theta = 1 - 0.26(\lambda/b)^2$. This equation has a solution only if $\lambda < 2.8b$. In Fig. 4 we have sharp maxima in $\sigma_I/\langle I\rangle$ for $\lambda = 10.5$ and $\lambda = 20.5$, but there are no sharp maxima for $\lambda = 50.5$. For CPHS clusters $b = 14.2$, and the critical value of λ is 39.7. We see that $\lambda = 50$ exceeds the critical value, and therefore the corresponding curve in Fig. 4 has no sharp maxima.

Now we analyze expression (42) in more detail. First, when $N \to \infty$, this expression assumes the form

$$\frac{\sigma_I}{\langle I\rangle} = \sqrt{\frac{2(1/\varphi^2 - 1)}{N}}. \tag{43}$$

As one could expect, the relative fluctuations are proportional to $1/\sqrt{N}$. In order to obtain Eq. (43), we need to require that $N\varphi^2 \gg 1$. It is important how this condition is expressed in terms of the density ν of monomers in clusters (where $N = 4\pi b^3\nu/3$). By using Eq. (38), we find that

$$\nu \gg \frac{1}{12\pi} q^3 \qquad \text{if } qb \sim 1, \tag{44}$$

$$\nu \gg \frac{(qb)}{12\pi} q^3 \qquad \text{if } qb \gg 1, \tag{45}$$

and the condition is always fulfilled if $qb \ll 1$, since $\varphi(0) = 1$. Note that in order to derive relations (44) and (45), we assumed that $\tan(qb) \neq qb$ and that $\sin(qb)$ and $\cos(qb) \sim 1$. As discussed above, if $\tan(qb) = qb$, then $\varphi(qb)$ turns exactly to zero and the condition $N\varphi^2 \gg 1$ cannot be fulfilled.

The inequalities show that in order to observe the $1/\sqrt{N}$ dependence for the fluctuations, one needs to have many monomers in the volume q^{-3}. This condition depends on the value of qb and is stronger when $qb \gg 1$. We want to emphasize that for fractal CCA clusters we never can obtain the $1/\sqrt{N}$ dependence for relative fluctuations (see, for example, the curve in Fig. 3 for $\lambda = 100.5$). The reason is that fractal clusters are disordered on all scales up to the maximum scale R_c, whereas trivial random clusters become homogeneous on scales larger than $1/\sqrt[3]{\nu}$.

Now we turn again to the nature of the sharp maxima in $\sigma_I/\langle I\rangle$ that are seen in Fig. 4(a). As mentioned in Subsection 5.A, these maxima coincide with the diffraction minima of the average scattered intensity. The reason for the diffraction minima is that, within the MFA and for certain scattering angles, the electric fields produced by monomers in a cluster almost exactly compensate each other on account of interference. As a result, the scattered field for these scattering angles is produced, in fact, by a very few monomers, rather than by the whole cluster. This results in the strong relative fluctuations.

In conclusion, we note that the theoretical expression (42) does not accurately fit the curves shown in Fig. 4(a), which were obtained from the numerical calculations for CPHS clusters. But it does fit the corresponding curves calculated numerically for totally uncorrelated random clusters (the results are not shown). This is explained by the above-mentioned fact that CPHS clusters are not absolutely uncorrelated, as a result of the repulsion of hard spheres at small distances.

6. DISCUSSION

The numerical and theoretical results obtained in Section 4 suggest that measuring fluctuations of the scattered light can provide additional valuable information about the nature and the properties of fractal pollutants in the atmosphere. One can use additional equations involving fluctuation characteristics to extract unknown parameters, such as the distribution of clusters over sizes, the average number of monomers in a cluster, and the density of clusters.

The fractal dimension of clusters and the average density of the material from which the clusters are built (e.g., soot) can be determined by measurement of the angular dependence of the average scattered intensity. However, these measurements would give no information on the degree of polydispersity of the clusters, their sizes, and the number of monomers that they contain.

We emphasize that the source of fluctuations studied in this paper is the random nature of fractal clusters. We did not consider such factors as atmospheric fluctuations, laser fluctuations, and broad mixtures of aerosols, which would play an important role in direct applications in the atmosphere. However, we can outline some possible schemes of measurements based on the geometrical properties of clusters.

By measuring fluctuations of the scattered light in the direction close to forward, one can obtain, according to Eqs. (22) and (37), the value of

$$\sqrt{\frac{\langle N^4\rangle - \langle N^2\rangle^2}{M\langle N^2\rangle^2}},$$

where M is the average number of clusters scattering the light. By measuring the same quantity at large scattering angles, one obtains the value of

$$\sqrt{\frac{2\sigma_N^2/\langle N\rangle^2 + 1}{M}}.$$

The quantity M can be excluded from these two expressions, so that only one expression remains, which provides some information about the distribution of N. Further, by adopting some theoretical distribution of N, one can calculate its parameters, such as the mean and the

dispersion. This, together with data on the average scattered intensity, can be used for the calculation of other parameters of the clusters.

This is only one of the possible ways in which fluctuation measurements can be employed. Another possibility is to measure fluctuations at some fixed scattering angle and to increase λ gradually until the dispersion begins to decrease (at $\lambda \approx 9R_{\mathrm{rms}}$; see the discussion at the end of Subsection 4.B). This can help to determine a characteristic geometrical size of clusters (see Subsection 4.B). In general, it is important that measurements of fluctuations provide additional relations between different parameters describing the clusters; these relations can be useful in a situation wherein the number of unknown parameters is larger than that of equations.

To summarize, we have shown that there are principal differences between fluctuations of light scattered by fractal and nonfractal (trivial) clusters. The main feature is that fluctuations in light scattering by fractals are typically much larger. The other is the dependence on the number of particles, N, in a cluster: Whereas for trivial clusters one expects the familiar $1/\sqrt{N}$ dependence (with certain limitations discussed in Subsection 5.B), this is not the case for fractal clusters, for which the $1/\sqrt{N}$ dependence can never be reached.

ACKNOWLEDGMENTS

This research was supported in part by the U.S. Environmental Protection Agency under grant R822658-01-0 and by the National Science Foundation under grant DMR-9500258.

Vadim A. Markel is also with the Institute of Automation and Electrometry, Siberian Branch of the Russian Academy of Science, 630090 Novosibirsk, Russia. Vladimir M. Shalaev is also with the L. V. Kirensky Institute of Physics, Siberian Branch of the Russian Academy of Science, 660036 Krasnoyarsk, Russia.

REFERENCES AND NOTES

1. J. P. Wolf, "3-D monitoring of air pollution using mobile all-solid-state Liar System," Opt. Photonics News **6,** 27–xx (1995).
2. N. Lu and C. M. Sorensen, "Depolarized light scattering from soot aggregates," Phys. Rev. E **50,** 3169–xxxx (1994).
3. K. A. Fuller, "Scattering and absorption cross sections of compounded spheres," J. Opt. Soc. Am. A **12,** 881–892 (1995).
4. N. G. Khlebtsov and A. G. Mel'nikov, "Depolarization of light scattered by fractal smoke clusters: an approximate anisotropic model," Opt. Spectrosc. **79,** 656–xxx (1995).
5. P. Qing, H. Nakane, Y. Sasano, and S. Kitamura, "Numerical simulation of the retrieval of aerosol size distribution from multiwavelength laser radar measurements," Appl. Opt. **28,** 5259–5265 (1989).
6. A. D. Papayannis, "The Eole Project—a multiwavelength laser remote-sensing (lidar) systems for ozone and aerosol measurements in the troposphere and the lower stratosphere. 1. Overview, Int. J. Remote Sensing **16,** 3595–xxxx (1996).
7. P. Chylek, V. Ramaswamy, R. Cheng, and R. G. Pinnik, "Optical properties and mass concentration of carbonaceous smokes," Appl. Opt. **20,** 2980–2985 (1981).
8. M. V. Berry and I. C. Percival, "Optics of fractal clusters such as smoke," Opt. Acta **33,** 577–591 (1986).
9. J. E. Martin and A. J. Hurd, "Scattering from fractals," J. Appl. Crystallogr. **20,** 61–xx (1987).
10. V. M. Shalaev, R. Botet, and R. Jullien, "Resonant light scattering by fractal clusters," Phys. Rev. B **44,** 12216–xxxxx (1991); **45,** 7592–xxxx (1992).
11. M. I. Stockman, L. N. Pandey, L. S. Muratov, and T. F. George, "Giant fluctuations of local fields in fractal clusters," Phys. Rev. Lett. **72,** 2486–xxxx (1994).
12. V. A. Markel, "Antisymmetrical optical states," J. Opt. Soc. Am. B **12,** 1783– (1995); V. A. Markel, V. M. Shalaev, E. B. Stechel, W. Kim, and R. L. Armstrong, "Small-particle composites. I. Linear optical properties, " Phys. Rev. B **53,** 2425–xxxx (1996).
13. R. Jullien and R. Botet, *Aggregation and Fractal Aggregates* (World Scientific, Singapore, 1987).
14. These parameters characterize the probability distribution according to which the values of N were picked for each cluster. The *actual* parameters of the ensemble were slightly different: $\langle N \rangle = 5343$ and $\sigma_N = 1953$.
15. J. D. Jackson, *Classical Electrodynamics* (Wiley, New York, 1975), Chap. 9.2.
16. Eigenvectors of a non-Hermitian symmetrical matrix are, in general, not orthogonal. However, it can be shown that $\langle \bar{m}|n \rangle = 0$ if $m \neq n$, where the bar denotes complex conjugation of all elements of a vector. We assume the usual normalization of the eigenvectors, $\langle n|n \rangle = 1$, but $\langle \bar{n}|n \rangle$ is not equal to 1 and can be complex.
17. As can be seen from Figs. 6 and 7, there is no real need in *strong* inequalities here.